AD-A113 530 NAVAL SURFACE WEAPONS CENTER SILVER SPRING MD F/G 20/7
THE INFLUENCE OF A BACKGROUND PLASMA ON THE DIOCOTRON INSTABILI--ETC(U)
SEP 81 H J BILOW, H S UHM
UNCLASSIFIED NSWC/TR-81-393 SBI-AD-F500 005 NL

1 OF 1
AD
A113530

END
DATE
FILMED
5-82
DTIC

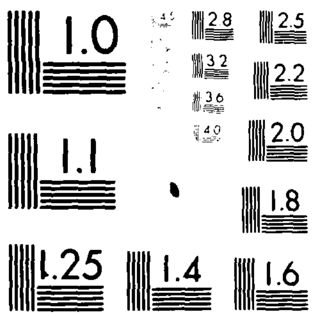

MICROCOPY RESOLUTION TEST CHART

AD-F500005

12

NSWC TR 81-393

AD A113530

THE INFLUENCE OF A BACKGROUND PLASMA ON THE DIOCOTRON INSTABILITY OF A RELATIVISTIC HOLLOW ELECTRON BEAM

BY HENRY J. BILOW HANS S. UHM

RESEARCH AND TECHNOLOGY DEPT.

SEPTEMBER 1981

NAVAL SURFACE WEAPONS CENTER

Dahlgren, Virginia 22448 • Silver Spring, Maryland 20910

UNCLASSIFIED

SECURITY CLASSIFICATION OF THIS PAGE (When Data Entered)

REPORT DOCUMENTATION PAGE		READ INSTRUCTIONS BEFORE COMPLETING FORM
1. REPORT NUMBER NSWC TR 81-393	2. GOVT ACCESSION NO. AD-A113 530	3. RECIPIENT'S CATALOG NUMBER
4. TITLE (and Subtitle) The Influence of a Background Plasma on the Diocotron Instability of a Relativistic Hollow Electron Beam		5. TYPE OF REPORT & PERIOD COVERED Final
		6. PERFORMING ORG. REPORT NUMBER
7. AUTHOR(s) Henry J. Bilow and Han S. Uhm		8. CONTRACT OR GRANT NUMBER(s)
9. PERFORMING ORGANIZATION NAME AND ADDRESS Naval Surface Weapons Center R41 White Oak, Silver Spring, Maryland 20910		10. PROGRAM ELEMENT, PROJECT, TASK AREA & WORK UNIT NUMBERS 61152N, ZR00001, ZR01109, 0
11. CONTROLLING OFFICE NAME AND ADDRESS		12. REPORT DATE September 1981
		13. NUMBER OF PAGES 39
14. MONITORING AGENCY NAME & ADDRESS(if different from Controlling Office)		15. SECURITY CLASS. (of this report) UNCLASSIFIED
		15a. DECLASSIFICATION/DOWNGRADING SCHEDULE

16. DISTRIBUTION STATEMENT (of this Report)

Approved for public release, distribution unlimited

17. DISTRIBUTION STATEMENT (of the abstract entered in Block 20, if different from Report)

18. SUPPLEMENTARY NOTES

19. KEY WORDS (Continue on reverse side if necessary and identify by block number)

Diocotron Instability
Hollow Electron Beam
Background Plasma
Relativistic Beam

20. ABSTRACT (Continue on reverse side if necessary and identify by block number)

The influence of a background plasma on the diocotron instability of a relativistic hollow electron beam is investigated within the framework of a cold fluid model. The background plasma is taken to have a uniform density except at the mean radius of the electron beam where the density is assumed to be discontinuous. Of the charged species comprising the plasma, only the electrons influence the dynamics of the beam-plasma system; the effect of the ions is negligible because of their small plasma frequency. A dispersion relation for the eigenfrequencies of the system is derived and employed to

DD FORM 1 JAN 73 1473 EDITION OF 1 NOV 65 IS OBSOLETE
S/N 0102-014-6601

UNCLASSIFIED

SECURITY CLASSIFICATION OF THIS PAGE (When Data Entered) examine instabilities. It is found that the fundamental ($\ell = 1$) mode, which is unconditionally stable for a hollow electron beam in a vacuum, is now unstable for certain parameter regimes. The appearance or growth of instabilities with increases in the plasma density discontinuity is observed, while increases in the relativistic factor γ_b are seen to exert a stabilizing influence. It is also found that thin beams are generally more unstable than thick ones.

FOREWORD

The influence of a background plasma on the diocotron instability of a relativistic hollow electron beam is investigated within the framework of a cold fluid model. The background plasma is taken to have a uniform density except at the mean radius of the electron beam where the density is assumed to be discontinuous. Of the charged species comprising the plasma, only the electrons influence the dynamics of the beam-plasma system; the effect of the ions is negligible because of their small plasma frequency. A dispersion relation for the eigenfrequencies of the system is derived and employed to examine instabilities. It is found that the fundamental (ℓ = 1) mode, which is unconditionally stable for a hollow electron beam in a vacuum, is now unstable for certain parameter regimes. The appearance or growth of instabilities with increases in the plasma density discontinuity is observed, while increases in the relativistic factor γ_b are seen to exert a stabilizing influence. It is also found that thin beams are generally more unstable than thick ones.

IRA M. BLATSTEIN
By direction

CONTENTS

ILLUSTRATIONS

INTRODUCTION

Numerous devices employing relativistic hollow electron beams, e.g., the coaxial autoaccelerator,[1] the free electron laser,[2,3] the relativistic magnetron,[4] and the gyrotron[5-7] are currently objects of study in diverse areas of research. A recent investigation[8] examined the stability of relativistic hollow electron beams in a vacuum. In this paper the investigation of stability is extended to include the case in which a background plasma is present. This case is of interest because any operating experimental device such as those listed above will contain a plasma produced by the ionization of the residual gas by the electron beam. If the density of this plasma is sufficiently great, its presence may have important consequences for the operation of the device since the beam parameters required for stable operation may be affected.

The analysis of the beam-plasma configuration will be carried out within the framework of a macroscopic cold fluid model, the temperatures of the beam electrons, plasma electrons, and plasma ions all being assumed negligible. Computation reveals that the ions, by virtue of their relatively small plasma frequency, can be neglected in the perturbation analysis employed in examining the stability of the beam-plasma configuration; the ions do affect the equilibrium state, however.

The analysis is restricted to the case where the electron beam is tenuous and where the electron density of the background plasma is no greater than that of the electron beam. In specifying a form for the density of the background plasma it is presumed that in a physical device this density would exhibit a gradient across the interior of the electron beam. For the sake of mathematical tractability this gradient will be accounted for by assuming that the plasma density is sharply discontinuous at a region inside the electron beam; elsewhere the plasma density is assumed to be uniform.

We shall begin by determining the equilibrium state of the beam-plasma configuration. The stability properties of the system will then be investigated through the use of a perturbation method employing the Maxwell-fluid equations. In particular we shall derive a dispersion relation for the eigenfrequencies of the perturbed configuration. Next this dispersion relation will be employed to investigate the stability properties of the configuration for various ranges of the parameters. It will be seen that the fundamental ($\ell = 1$) mode can be unstable, in contradistinction to the vacuum case where this mode is unconditionally stable. It will also be observed that increases in the plasma density discontinuity or decreases in the beam thickness are generally destabilizing, whereas increases in the relativistic factor γ_b have a stabilizing effect.

BEAM-PLASMA CONFIGURATION AT EQUILIBRIUM

Figure 1 illustrates the configuration of the electron beam and the background plasma at equilibrium. With reference to the cylindrical coordinate system shown in Figure 1, the beam is seen to be propagating with uniform velocity $\beta_b c\hat{e}_z$ and is coaxial with a perfectly conducting outer cylinder of radius R_c. R_1 and R_2 are, respectively, the inner and outer radii of the hollow electron beam. A uniform axial applied magnetic field, $B_0\hat{e}_z$, is assumed to be present to provide radial confinement of the beam.

The equilibrium electron density profile of the beam and of the plasma, $n_b^0(r)$ and $n_e^0(r)$ respectively, are illustrated in Figure 2. Both profiles are assumed to be independent of θ. The beam electron density is taken to be uniform across the width of the beam and to fall sharply to zero at the beam edges. The plasma electron density is taken to be piecewise uniform, undergoing a discontinuous decrease by a factor α at the midpoint of the electron beam from its value at the beam axis. The plasma is assumed to be electrically neutral at equilibrium so that each ion density profile of the various ion species would have the same form as that of the plasma electrons. The equilibrium electron densities may be written as

$$n_b^0(r) = n_{b0}[U(r - R_1) - U(r - R_2)] \ , \qquad (1)$$

$$n_p^0(r) = n_{e0}[U(r) - (1 - \alpha)U(r - R_p)] \ , \qquad (2)$$

where $R_p = (R_1 + R_2)/2$, where $U(r)$ is a unit step function (Heaviside function), where n_{b0} and n_{e0} are constants, and where the parameter α satisfies $0 \leq \alpha \leq 1$.

In analyzing the equilibrium configuration the following additional assumptions are made:

i) All of the beam and plasma variables are azimuthally symmetric, i.e., $\partial/\partial\theta = 0$. The azimuthal motion of the beam will thus be laminar.

ii) The beam-plasma configuration is infinitely long with no axial variations, i.e., $\partial/\partial z = 0$.

iii) The beam and plasma charged particles are in slow rotational equilibrium with mean azimuthal velocities equal to $\underset{\sim}{E} \times \underset{\sim}{B}$ drift velocities.

iv) The azimuthal momenta of the charged particles are non-relativistic and small compared to the axial momentum of the beam electrons.

v) The beam electron density is assumed to be such that the following inequalities are satisfied:

$$\hat{\omega}_{pb}^2 << \omega_{cb}^2 , \tag{3}$$

$$\sqrt{\omega_{cj}\omega_{ce}} << \hat{\omega}_{pb} . \tag{4}$$

Here $\hat{\omega}_{pb}^2 \equiv 4\pi e^2 n_{b0}/\gamma_b m_e$ is the square of the beam electron plasma frequency, where $\gamma_b \equiv 1/\sqrt{1 - \beta_b^2}$; $\omega_{cb} \equiv eB_0/\gamma_b m_e c$ is the beam electron cyclotron frequency; $\omega_{ce} = \gamma_b \omega_{cb}$ is the plasma electron cyclotron frequency; and $\omega_{cj} \equiv q_j B_0/m_j c$ is the cyclotron frequency of the jth species of ions, where q_j is the ionic charge. Inequality (3) implies that the electron beam is tenuous, while (4) states that the beam is nevertheless sufficiently dense so that the lower hybrid frequency of the plasma is much less than the plasma frequency of the beam electrons.

As stated earlier, the analysis will be carried out within the framework of a cold fluid model. The equations of motion and continuity which ch[illegible]acterize [illegible]he μth component of the fluid (beam electrons, plasma electrons, or the jth species of ions) are then

$$\left(\frac{\partial}{\partial t} + \underset{\sim}{V}_\mu \cdot \nabla\right)\gamma_\mu m_\mu \underset{\sim}{V}_\mu = \varepsilon_\mu q_\mu \left(\underset{\sim}{E} + \frac{1}{c}\underset{\sim}{V}_\mu \times \underset{\sim}{B}\right) , \tag{5}$$

$$\frac{\partial}{\partial t} n_\mu + \nabla \cdot (n_\mu \underset{\sim}{V}_\mu) = 0 , \tag{6}$$

where $\underset{\sim}{E}$ and $\underset{\sim}{B}$, respectively, the electric and magnetic fields; where n_μ and $\underset{\sim}{V}_\mu$ are the number density and velocity, respectively, of the fluid component; where m_μ and q_μ are, respectively, the mass and charge magnitude of the particles comprising the fluid component; where ε_μ is the sign of the charge of the fluid component particles; and where γ_μ is the relativistic factor $(1 - \underset{\sim}{V}_\mu \cdot \underset{\sim}{V}_\mu/c^2)^{-1/2}$ for the particles of the fluid component (γ_μ is essentially unity except for the beam electron component).

The electromagnetic field is governed by Maxwell's equations

$$\nabla \times \underset{\sim}{E} = -\frac{1}{c}\frac{\partial}{\partial t}\underset{\sim}{B} , \tag{7a}$$

$$\nabla \times \underset{\sim}{B} = \frac{4\pi}{c}\underset{\sim}{J} + \frac{1}{c}\frac{\partial}{\partial t}\underset{\sim}{E} , \tag{7b}$$

$$\nabla \cdot \underset{\sim}{E} = 4\pi\rho , \tag{7c}$$

where ρ and $\underset{\sim}{J}$ are the charge and current densities, respectively. The electric and magnetic fields can be derived from potentials ϕ and $\underset{\sim}{A}$,

$$\underset{\sim}{E} = -\nabla\phi - \frac{1}{c}\frac{\partial}{\partial t}\underset{\sim}{A} , \tag{8}$$

$$\underset{\sim}{B} = \nabla \times \underset{\sim}{A} + B_0 \underset{\sim}{\hat{e}}_z . \tag{9}$$

These potentials satisfy

$$\left(\nabla^2 - \frac{1}{c^2}\frac{\partial^2}{\partial t^2}\right)\phi = -4\pi\rho \ , \tag{10a}$$

$$\left(\nabla^2 - \frac{1}{c^2}\frac{\partial^2}{\partial t^2}\right)\underset{\sim}{A} = -\frac{4\pi}{c}\underset{\sim}{J} \ . \tag{10b}$$

At equilibrium, consistent with the assumptions stated earlier, we have

$$n_\mu = n_\mu^0(r) \ , \tag{11}$$

$$\underset{\sim}{V}_\mu = V_{\mu\theta}^0(r)\underset{\sim}{\hat{e}}_\theta + \beta_\mu c\underset{\sim}{\hat{e}}_z \ , \tag{12}$$

$$\phi = \phi^0(r) \ , \tag{13}$$

$$\underset{\sim}{A} = A_z^0(r)\underset{\sim}{\hat{e}}_z \ , \tag{14}$$

where the superscript zero denotes the equilibrium form of the associated quantity. The following also apply at equilibrium:

$$\rho = -en_b^0 \ , \tag{15}$$

$$\underset{\sim}{J} = -\beta_b c e n_b^0 \underset{\sim}{e}_z \ , \tag{16}$$

where n_b^0 is given by Eq. (1). By employing the technique of Uhm and Siambis[8] the following expressions are obtained for the equilibrium rotational velocities $\omega_\mu^0 \equiv V_{\mu\theta}^0/r$ of the electrons in slow rotation:

$$\omega_b^0(r) \equiv \omega_D[1 - (R_1/r)^2]U(r - R_1) \ , \tag{17a}$$

for the beam electrons, and

$$\omega_p^0(r) \equiv \gamma_b^2\omega_D\{[1 - (R_1/r)^2]U(r - R_1) - [1 - (R_2/r)^2]U(r - R_2)\} , \qquad (17b)$$

for the plasma electrons, where ω_D is the diocotron frequency,

$$\omega_D \equiv \hat{\omega}_{pb}^2/2\gamma_b^2\omega_{cb} . \qquad (18)$$

It can also be shown that

$$\omega_j^0 = O(\omega_p^0) , \qquad (19)$$

for the plasma ions in slow rotation; the explicit form of the ion rotational velocities will not be needed.

PERTURBATION ANALYSIS

The stability of the electron beam-plasma configuration will be examined by applying a perturbation analysis to linearized equations of motion and continuity. In the perturbation analysis a typical quantity of interest, e.g., charge density ρ, is written as

$$\rho(\underset{\sim}{r},t) = \rho^0(r) + \delta\rho(\underset{\sim}{r},t) \ , \tag{20}$$

where ρ^0 is the equilibrium charge density and $\delta\rho$ the perturbed charge density. In the stability analysis all of the perturbed quantities are Fourier decomposed in a manner typified by

$$\delta\rho(\underset{\sim}{r},t) = \delta\rho_\ell(r,\theta)\exp[i(\ell\theta - \omega t)] \ , \tag{21}$$

where ℓ is the azimuthal harmonic number and ω is the eigenfrequency. Using the perturbed quantities $\delta\rho_\ell$, etc., a dispersion relation will be derived for the eigenfrequencies. By solving this dispersion relation for the eigenfrequencies the stability properties of the configuration can be determined.

The first step in the perturbation analysis is the determination of the perturbed electric and magnetic fields $\delta\underset{\sim}{E}$, $\delta\underset{\sim}{B}$. These fields can be derived from perturbed potentials $\delta\phi$, $\delta\underset{\sim}{A}$ in the manner shown in Eqs. (8) and (9) (except that the constant term $B_0\underset{\sim}{\hat{e}}_z$ in Eq. (9) is now dropped). The perturbed potentials, together with perturbed source terms, satisfy relationships given by Eqs. (10a,b).

The stability analysis is restricted to frequencies satisfying

$$|\omega R_c| \ll \ell c \ . \tag{22}$$

With this restriction the following are obtained from Eqs. (10a,b) for the perturbed potentials:

$$\left(\frac{1}{r}\frac{\partial}{\partial r} r \frac{\partial}{\partial r} - \frac{\ell^2}{r^2}\right) \delta\phi_\ell(r,\omega) = -4\pi\delta\rho_\ell(r,\omega) \ , \tag{23a}$$

$$\left(\frac{1}{r}\frac{\partial}{\partial r} r \frac{\partial}{\partial r} - \frac{\ell^2}{r^2}\right) \delta A_{z\ell}(r,\omega) = -\frac{4\pi}{c}\,\delta J_{z\ell}(r,\omega) \ . \tag{23b}$$

In Eq. (31b) $\delta J_{z\ell}$ and $\delta A_{z\ell}$ are the z-components of the perturbed current density and vector potential, respectively. Because the azimuthal velocities of the components of the beam-plasma configuration are assumed to be nonrelativistic, the forces resulting from the magnetic field generated by the azimuthal current are negligible.[9] Hence only the axial components of the perturbed current density and perturbed vector potential are needed in the analysis.

By virtue of the foregoing considerations the perturbed electromagnetic field can be obtained from the perturbed potentials as follows:

$$\delta E_{r\ell}(r,\omega) = -\frac{\partial}{\partial r}\,\delta\phi_\ell(r,\omega) \ , \tag{24a}$$

$$\delta E_{\theta\ell}(r,\omega) = -\frac{i\ell}{r}\,\delta\phi_\ell(r,\omega) \ , \tag{24b}$$

$$\delta B_{r\ell}(r,\omega) = \frac{i\ell}{r}\,\delta A_{z\ell}(r,\omega) \ , \tag{24c}$$

$$\delta B_{\theta\ell}(r,\omega) = -\frac{\partial}{\partial r}\,\delta A_{z\ell}(r,\omega) \ . \tag{24d}$$

The equations of motion and continuity for the perturbed fluid variables are obtained by linearizing Eqs. (5) and (6) about the equilibrium values of these variables, neglecting terms higher than first order. The results for the equation of motion are

$$-i(\omega - \ell\omega_\mu^0)\delta V_{r\mu\ell} - (2\omega_\mu^0 + \omega_{c\mu})\delta V_{\theta\mu\ell}$$

$$= -\frac{\epsilon_\mu q_\mu}{\gamma_\mu m_\mu}\frac{\partial}{\partial r}(\delta\phi_\ell - \beta_\mu \delta A_{z\ell}) \ , \tag{25a}$$

$$\left[\omega_\mu^0 + \frac{\partial}{\partial r}(r\omega_\mu^0) + \omega_{c\mu}\right]\delta V_{r\mu\ell} - i(\omega$$

$$- \ell\omega_\mu^0)\delta V_{\theta\mu\ell} = -\frac{\epsilon_\mu q_\mu}{\gamma_\mu m_\mu}\frac{i\ell}{r}(\delta\phi_\ell - \beta_\mu \delta A_{z\ell}) \ , \tag{25b}$$

while for the equation of continuity the following is obtained:

$$-i(\omega - \ell\omega_\mu^0)\delta n_\mu + n_\mu^0\left(\frac{1}{r}\frac{\partial}{\partial r}(r\delta V_{r\mu\ell})\right.$$

$$\left. + \frac{i\ell}{r}\delta V_{\theta\mu\ell}\right) + \left(\frac{\partial}{\partial r}n_\mu^0\right)\delta V_{r\mu\ell} = 0 \ . \tag{26}$$

In these expressions the subscript μ indicates the component of the configuration (beam electrons, plasma electrons, or one of the ion species); the symbol $\omega_{c\mu}$ denotes the cyclotron frequency of the component.

The perturbation solution proceeds by solving Eqs. (25a,b) and (26) for the perturbed number densities in terms of the perturbed potentials. By employing the resulting expressions for the perturbed number densities in the relations

$$\delta\rho_\ell = \sum_\mu \epsilon_\mu q_\mu \delta n_\mu \ , \tag{27a}$$

$$\delta J_{z\ell} = -e\beta_b c\delta n_b \ , \tag{27b}$$

we can obtain expressions for the perturbed charge and current densities in terms of the perturbed potentials.

The expressions for the perturbed charge and current densities in terms of the perturbed potentials are employed in Eqs. (23a,b) in order to obtain a pair of coupled differential equations for the perturbed potentials. These differential equations can be considerably simplified by employing inequalities (3) and (4). In particular, the effects of the ions can be shown to be negligible in comparison to those of the beam and plasma electrons. The influence of these latter two components depends principally on terms with the coefficients $\frac{\partial}{\partial r}\omega_{pb}^2$, $\frac{\partial}{\partial r}\omega_{pe}^2$ where

$$\omega_{pb}^2 \equiv 4\pi e^2 n_b^0/\gamma_b m_e \ , \qquad (28a)$$

$$\omega_{pe}^2 \equiv 4\pi e^2 n_e^0/m_e \ ; \qquad (28b)$$

use of Eqs. (1) and (2) then leads to

$$\frac{\partial}{\partial r}\omega_{pb}^2 = \hat{\omega}_{pb}^2[\delta(r - R_1) - \delta(r - R_2)] \ , \qquad (29a)$$

$$\frac{\partial}{\partial r}\omega_{pe}^2 = -(1-\alpha)\hat{\omega}_{pe}^2\delta(r - R_p) \ , \qquad (29b)$$

where $\hat{\omega}_{pe}^2$ is the square of the plasma frequency

$$\hat{\omega}_{pe}^2 \equiv 4\pi e^2 n_{e0}/m_e \ . \qquad (30)$$

After defining the generalized potentials

$$\delta\psi_\ell \equiv \delta\phi_\ell - \beta_b\delta A_{z\ell} \ , \qquad (31a)$$

$$\delta\zeta_\ell \equiv \beta_b^2\delta\phi_\ell - \beta_b\delta A_{z\ell} \ , \qquad (31b)$$

the following set of coupled differential equations are obtained

$$\left(\frac{1}{r}\frac{\partial}{\partial r}\, r\, \frac{\partial}{\partial r} - \frac{\ell^2}{r^2}\right)\delta\psi_\ell = -\frac{\ell(1-\alpha)\gamma_b^2\hat{\omega}_{pe}^2\,\delta(r - R_p)}{\omega_{ce} r(\omega - \ell\omega_p^0)}\,(\delta\zeta_\ell - \delta\psi_\ell) - \frac{2\ell\omega_D[\delta(r - R_1) - \delta(r - R_2)]}{r(\omega - \ell\omega_b^0)}\,\delta\psi_\ell\,, \tag{32a}$$

$$\left(\frac{1}{r}\frac{\partial}{\partial r}\, r\, \frac{\partial}{\partial r} - \frac{\ell^2}{r^2}\right)\delta\zeta_\ell = -\frac{\ell(1-\alpha)\beta_b^2\gamma_b^2\hat{\omega}_{pe}^2\,\delta(r - R_p)}{\omega_{ce} r(\omega - \ell\omega_p^0)}\,(\delta\zeta_\ell - \delta\psi_\ell). \tag{32b}$$

DISPERSION RELATION

A dispersion relation for the eigenfrequencies of the beam-plasma configuration can be derived by solving Eqs. (32a,b) after imposing the boundary conditions that $\delta\psi_\ell$, $\delta\zeta_\ell$ are finite at $r = 0$ and vanish at $r = R_c$. The derivation of this relation will now be outlined briefly.

First, we note that the right-hand sides of Eqs. (32a,b) vanish except at $r = R_1$, R_p, R_2; for r not equal to any of these values the solutions for $\delta\psi_\ell$, $\delta\zeta_\ell$ will both have the form $ar^m + a'r^{-m}$ where a,a' are independent of r. Therefore, the r-interval $(0,R_c)$ is divided into four subintervals $(0,R_1)$, (R_1, R_p), (R_p, R_2), (R_2, R_c), and the solutions for $\delta\psi_\ell$, $\delta\zeta_\ell$ in each of these subintervals are written as

$$\delta\psi_\ell = a_k r^\ell + a_k' r^{-\ell} \tag{33a}$$

$$\delta\zeta_\ell = b_k r^\ell + b_k' r^{-\ell} , \tag{33b}$$

where the subscript k indicates the subinterval ($k = 1,2,3,4$).

Now the potentials $\delta\psi_\ell$, $\delta\zeta_\ell$ are continuous functions of r at the points $r = R_1$, R_p, R_2. The r-derivatives of the potentials are discontinuous at these points by quantities which are obtained by integrating Eqs. (32a,b) with respect to r over infinitesimal intervals centered at these points. For instance, the integration of Eq. (32a) from $r = R_1^-$ to $r = R_1^+$ yields

$$\frac{\partial}{\partial r}\,\delta\psi_\ell(r,\omega)\bigg|_{r=R_1^+} - \frac{\partial}{\partial r}\,\delta\psi_\ell(r,\omega)\bigg|_{r=R_1^-} = -\,\frac{2\ell\omega_D}{R_1[\omega - \ell\omega_b^0(R_1)]}\,\delta\psi_\ell(R_1,\omega) \;. \tag{34}$$

By using this and similar results at $r = R_p$, R_2, and by employing the boundary conditions, we obtain, after some tedious algebra, the dispersion relation

$$d_3(\omega/\omega_D)^3 + d_2(\omega/\omega_D)^2 + d_1(\omega/\omega_D) + d_0 = 0 \;, \tag{35}$$

where

$$d_3 \equiv (\xi_{c2} - 1)(1 - \xi_{cp}) \;, \tag{36a}$$

$$d_2 \equiv [\xi_{12} - \ell(\xi_{c2} - 1)(\lambda_2 + \lambda_p)](1 - \xi_{cp})$$
$$+ \gamma_b^4\lambda_\alpha[\beta_b^2\xi_{cp}(\xi_{c2} - 1) + (1 - \xi_{cp})(\xi_{c2} - \xi_{p2})] \;, \tag{36b}$$

$$d_1 \equiv [\ell^2(\xi_{c2} - 1)\lambda_p\lambda_2 - \ell\xi_{12}\lambda_p - \ell(\xi_{12} - \xi_{c2})\lambda_2$$
$$- \xi_{c2}\xi_{12}](1 - \xi_{cp}) + \gamma_b^4\lambda_\alpha[\beta_b^2\xi_{cp}\{\xi_{12}$$
$$- \ell(\xi_{c2} - 1)\lambda_2\} + \{\xi_{c2}\xi_{p2} - \ell(\xi_{c2} - \xi_{p2})\lambda_2$$
$$- (\xi_{c2} - \xi_{p2})\xi_{1p}\}(1 - \xi_{cp})] \;, \tag{36c}$$

$$d_0 \equiv \ell[\ell(\xi_{12} - \xi_{c2})\lambda_2 + \xi_{c2}\,\xi_{12}](1 - \xi_{cp})\lambda_p$$
$$+ \gamma_b^4\lambda_\alpha[\{\ell(\xi_{c2} - \xi_{p2})\lambda_2 - \xi_{c2}\xi_{p2}\}(1$$
$$- \xi_{cp})\xi_{1p} + \beta_b^2\xi_{cp}\{\ell(\xi_{c2} - \xi_{12})\lambda_2$$
$$- \xi_{c2}\xi_{12}\}] \;, \tag{36d}$$

and where

$$\xi_{\mu\nu} \equiv 1 - (R_\mu/R_\nu)^{2\ell} , \tag{37a}$$

$$\lambda_2 \equiv \omega_b^0(R_2)/\omega_D , \tag{37b}$$

$$\lambda_p \equiv \omega_p^0(R_p)/\omega_D , \tag{37c}$$

$$\lambda_\alpha \equiv (1-\alpha)n_{p0}/n_{b0} . \tag{37d}$$

It is significant to note that the plasma parameter α and the equilibrium electron densities enter into the dispersion relation coefficients d_i solely through the parameter λ_α given by Eq. (37d). The other parameters in these coefficients depend only on the geometric quantities R_1, R_2, R_p, R_c, and on the relativistic quantities γ_b, β_b.

RESULTS

The dispersion relation given by Eq. (35) has been employed to study the stability of the electron beam-plasma configuration for a substantial range of parameter variation. In the following are presented the most significant results from this study.

One of the first observations was the appearance of an instability in the $\ell = 1$ mode for certain parameter regimes. This contrasts sharply with the unconditional stability of this mode in the absence of plasma.[8] In Fig. 3 is plotted the region of instability in the $(R_1/R_2, \lambda_\alpha)$ parameter space for $\gamma_b = 2$ and $R_2/R_c = 0.8$. The growth in the area of the unstable range of R_1/R_2 with increasing λ_α is evident. It is also observed from additional numerical studies that increases in γ_b cause the unstable region to shrink, and that generally, the thinner the electron beam, i.e., the closer R_1/R_2 is to unity, the larger the unstable range in λ_α. This last property is found to be true for all modes.

It is also of interest to examine the stability in the $(R_1/R_2, R_2/R_c)$ parameter space for a fixed λ_α for the $\ell = 1$ mode. Numerical studies show that the appearance of an instability is usually more sensitive to changes in the ratio R_1/R_2 than to changes in the R_2/R_c ratio. It is again found that the unstable region shrinks with increases in γ_b.

The decreases in the areas of the unstable regions in the $(R_1/R_2, \lambda_\alpha)$ and $(R_1/R_2, R_2/R_c)$ parameter spaces with increases in γ_b appear to be unique to the $\ell = 1$ mode. For the higher modes the converse behavior is generally the rule.

The shape of the unstable region in the $(R_1/R_2, R_2/R_c)$ parameter space for the $\ell = 2$ mode is found to differ considerably from those of the $\ell = 1$ and $\ell > 2$ modes. The shape of the unstable region for $\ell = 2$ is shown in Fig. 4; the relevant parameters are $\gamma_b = 5$ and $\lambda_\alpha = 0.5$. In Fig. 4 it can be seen that the appearance of an instability can be very sensitive to the R_2/R_c ratio.

The areas of the unstable regions are found to decrease as the mode index increases. In Fig. 5 is shown the shape of the unstable region in the $(R_1/R_2, \lambda_\alpha)$ parameter space for the $\ell = 3$ mode and for $\gamma_b = 5$, $R_2/R_c = 0.8$. As the mode index is increased while the other parameters $(\gamma_b, R_2/R_c)$ are held constant, the extreme left-hand boundary of the unstable region is found to move to the right.

This section on results is concluded with an examination of the behavior of the eigenfrequencies with parameter variations. In Fig. 6 are plotted the real and imaginary parts of the normalized (with respect to ω_D) eigenfrequencies for several modes for varying λ_α. The parameters for these plots are $\gamma_b = 5$, $R_1/R_2 = 0.75$, and $R_2/R_c = 0.8$. It is evident that the growth rates of the instabilities, i.e., the imaginary components of the eigenfrequencies, increase as λ_α increases for all except the $\ell = 2$ mode. Thus we see that the greater the plasma electron density discontinuity, the more unstable the beam-plasma configuration.

The effect of relative beam thickness on the eigenfrequencies is typified by the plots of Fig. 7, which illustrate the variations in the growth rates of the instabilities with relative beam thickness for beam-plasma parameters of $\gamma_b = 5$, $R_2/R_c = 0.8$, and $\lambda_\alpha = 1.0$. It is evident that as the relative beam thickness decreases from maximum $(R_1/R_2 = 0)$ the number of unstable modes and the peak growth rates increase, reach maximum values, and then fall to zero as the beam thickness approaches zero. Thin beams are seen to be more unstable, in general, than thick beams.

Finally, additional numerical studies show that while normalized growth rates tend to increase as γ_b increases, the absolute growth rates decline by virtue of the normalization factor ω_D being inversely proportional to γ_b^2.

CONCLUSIONS

The stability of a relativistic hollow electron beam propagating through a background plasma with a step discontinuity has been analyzed within the framework of a cold fluid model. The analysis began with the solving for the equilibrium state of the beam-plasma configuration (Sec. II), after which a perturbation technique was employed with linearized equations of motion to derive differential equations for generalized field potentials (Sec. III). A dispersion relation for the eigenfrequencies of the configuration was then obtained (Sec. IV) and was used to examine the stability properties. The significant findings include the appearance of an instability in the $\ell = 1$ mode, which is stable in the absence of plasma; the generally more unstable nature of thin beams as opposed to thick ones; the stabilizing influence of large values of γ_b; and the increase in the growth rates of the instabilities (except for the $\ell = 2$ mode) with increases in the plasma density discontinuity.

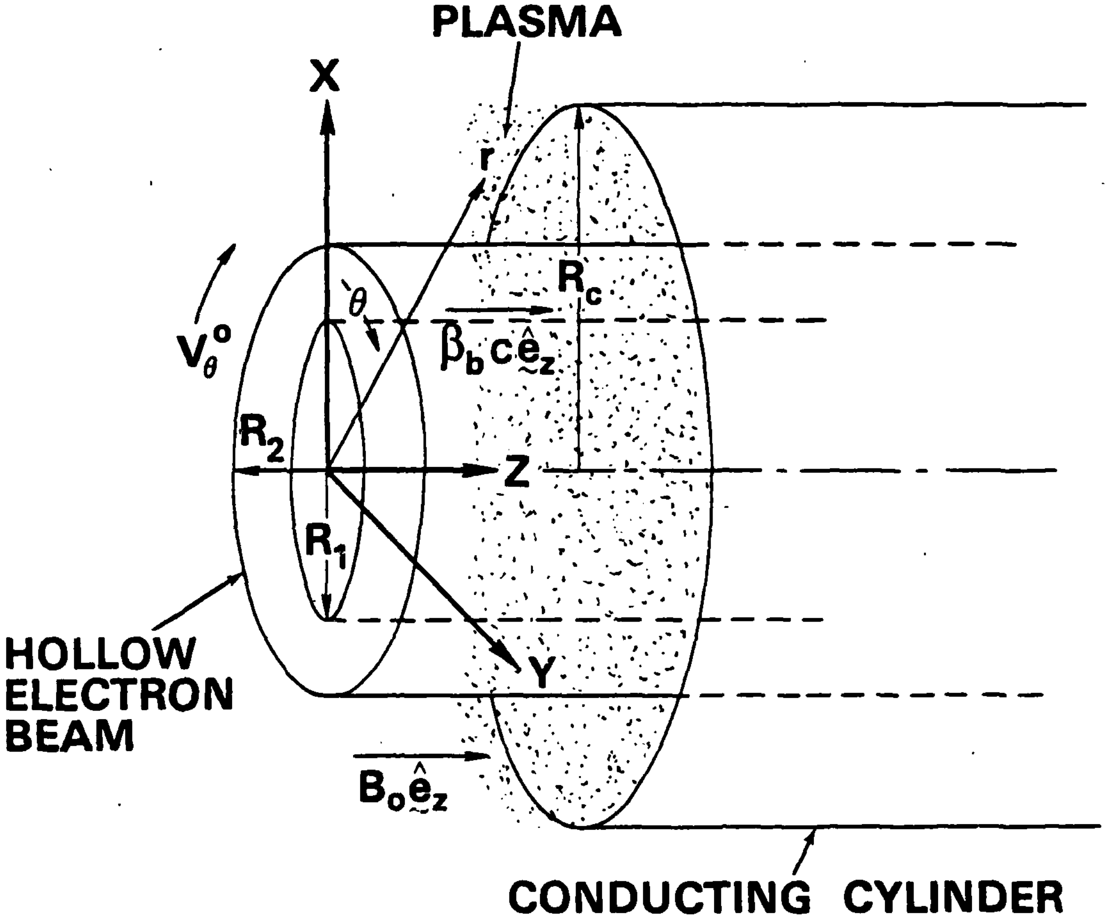

Fig. 1 Electron beam-plasma configuration and coordinate system

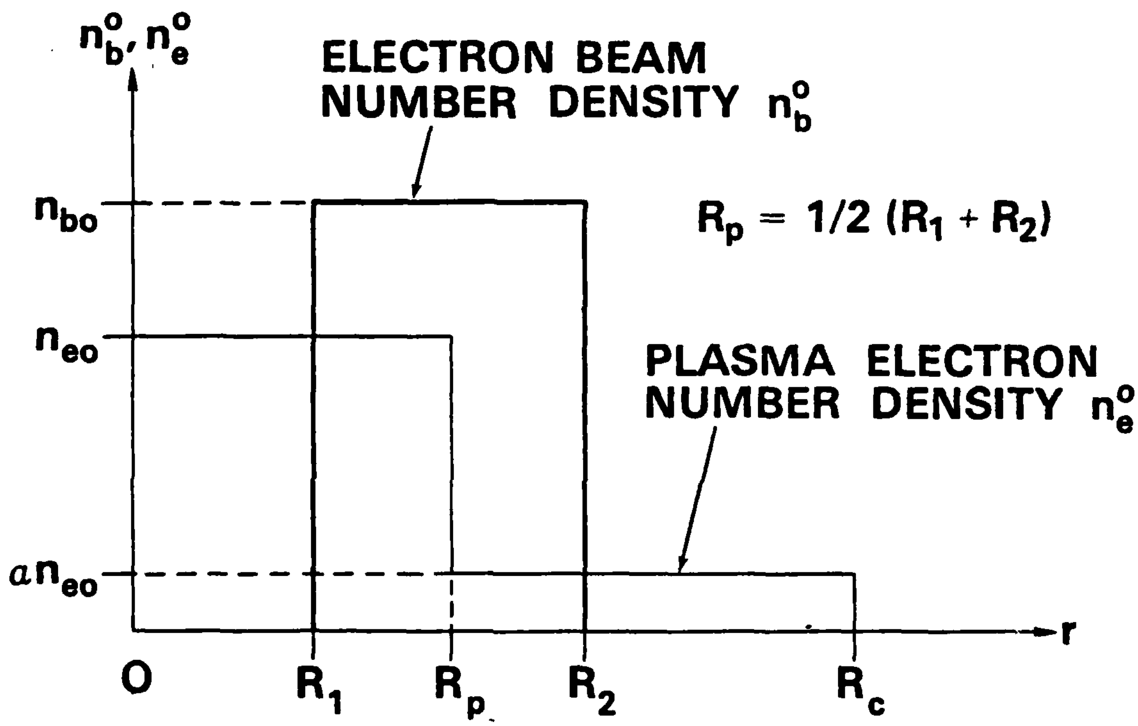

Fig. 2 Electron number density profiles of electron beam and plasma at equilibrium

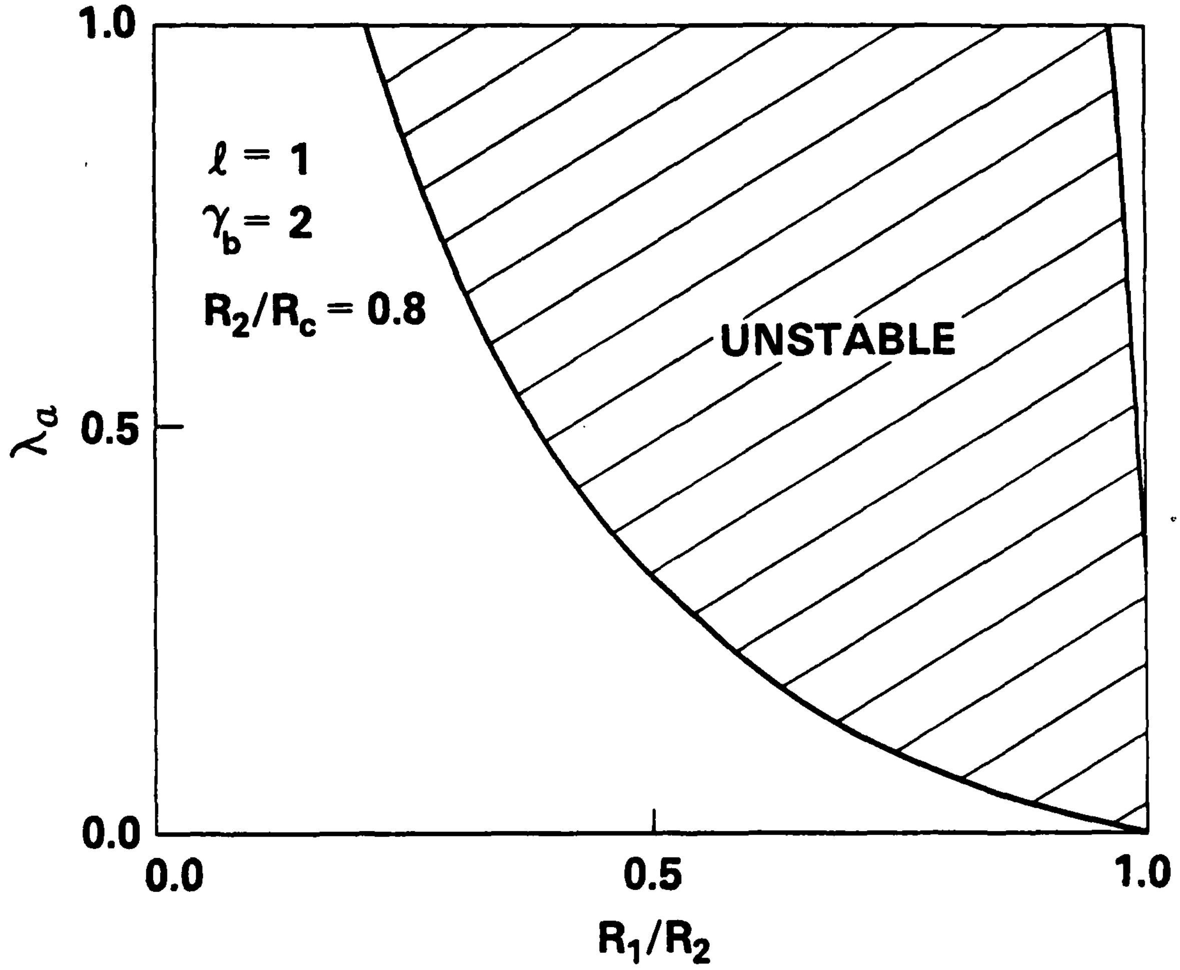

Fig. 3 Instability region in the (R_1/R_2, λ_α) parameter space for the ℓ = 1 mode for R_2/R_c = 0.8 and γ_b = 2

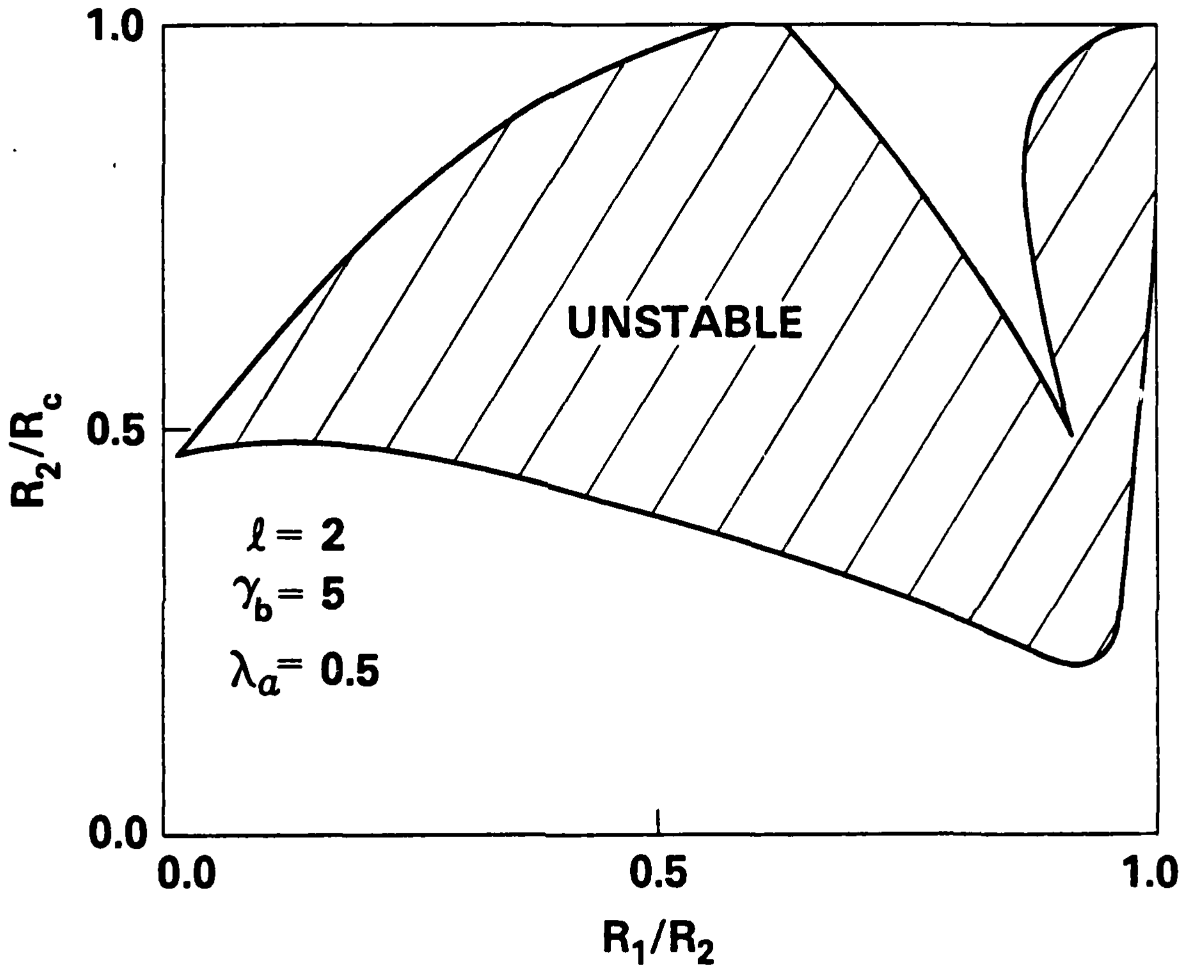

Fig. 4 Instability region in the (R_1/R_2, R_2/R_c) parameter space for the $\ell = 2$ mode when $\gamma_b = 5$ and $\lambda_a = 0.5$

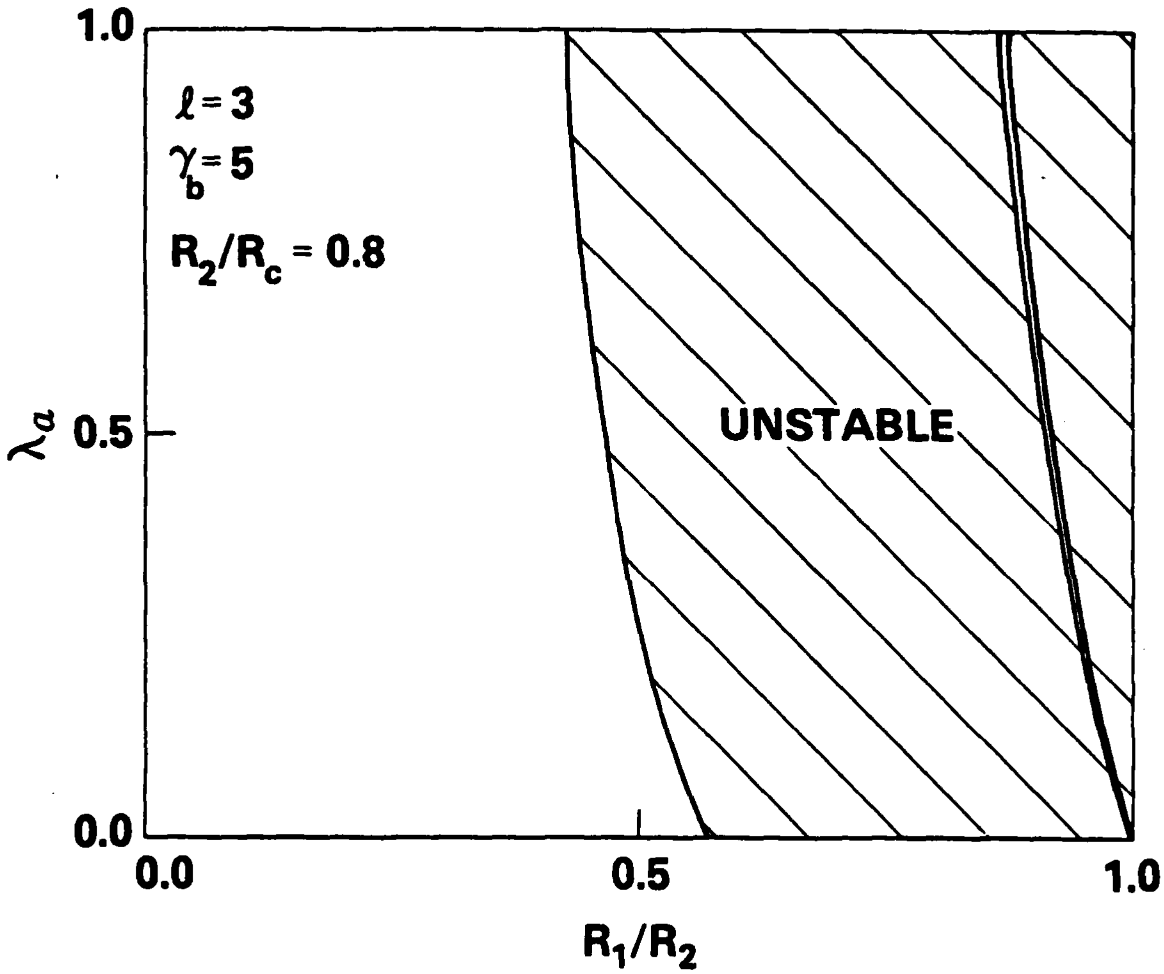

Fig. 5 Instability region in the $(R_1/R_2, \lambda_\alpha)$ parameter space for the $\ell = 3$ mode for $R_2/R_c = 0.8$ and $\gamma_b = 5$

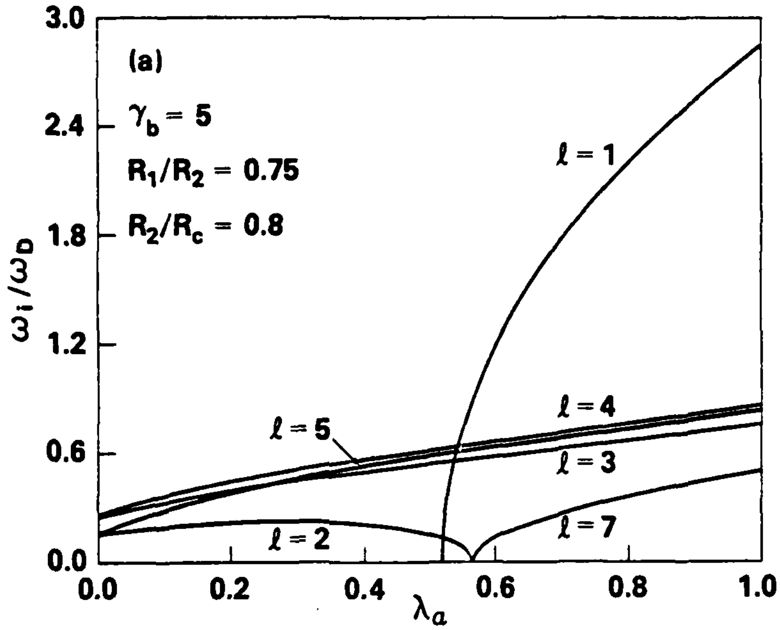

(a)

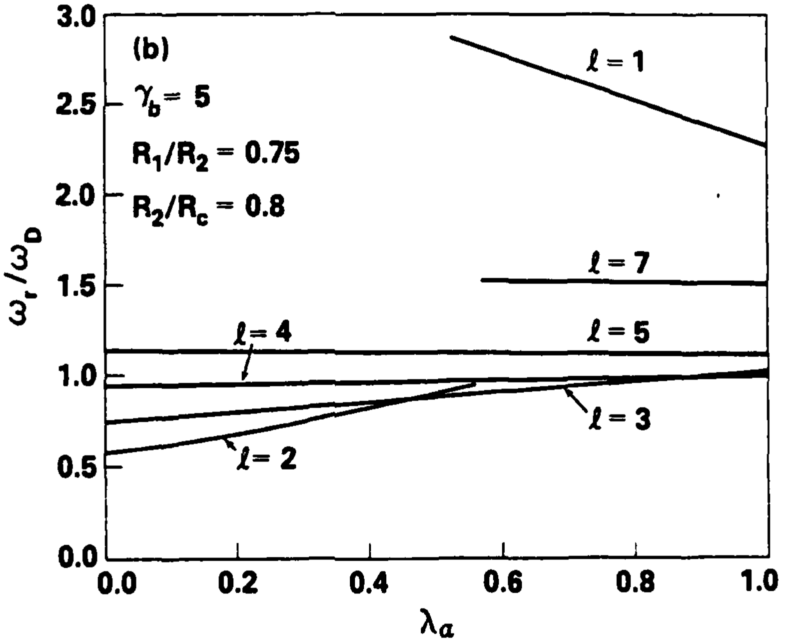

(b)

Fig. 6 Dependence of the normalized eigenfrequencies on the λ_a parameter for several modes for $\gamma_b = 5$, $R_1/R_2 = 0.75$, and $R_2/R_c = 0.8$: a) imaginary components and b) real components of the normalized eigenfrequencies

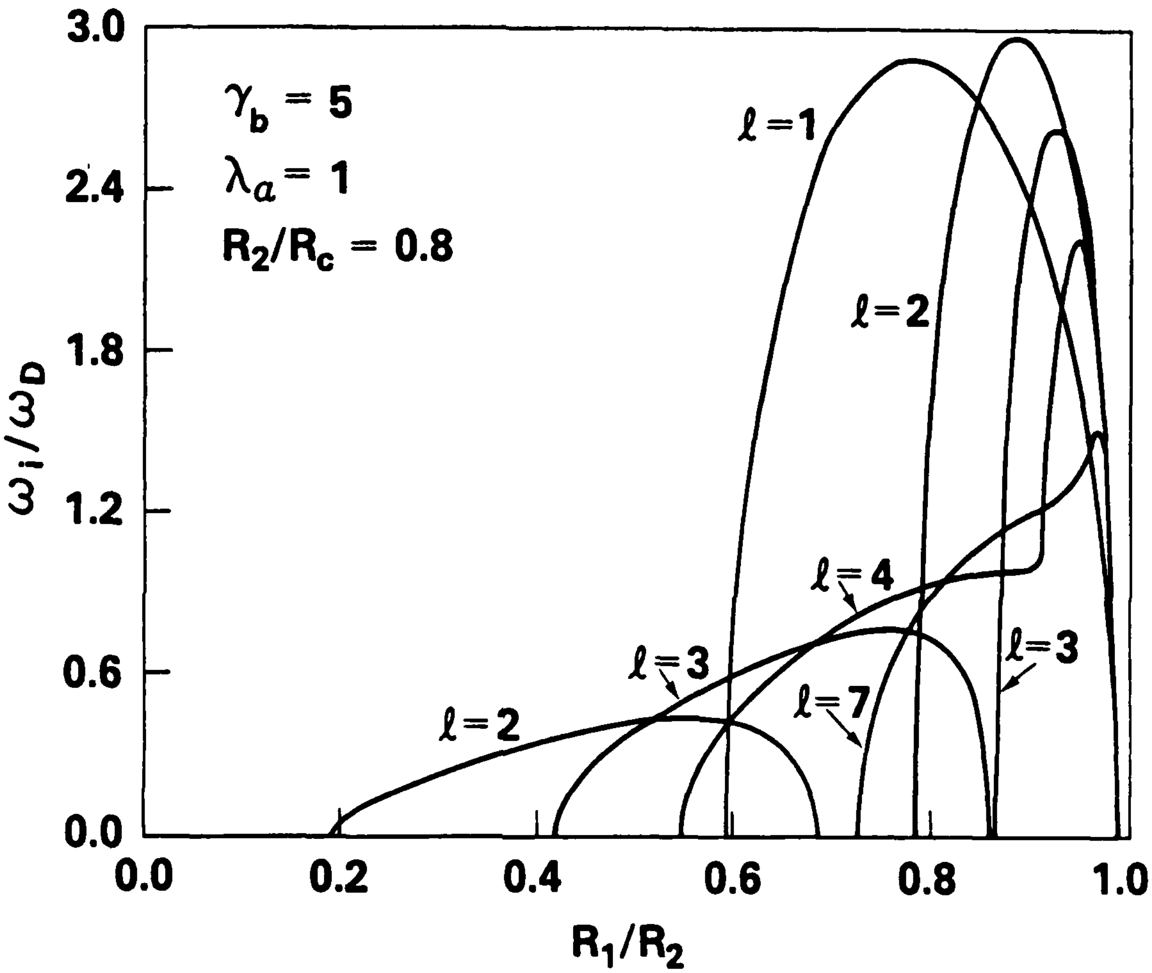

Fig. 7 Dependence of the normalized growth rates on relative beam thickness for several modes for $\gamma_b = 5$, $\lambda_\alpha = 1$, and $R_2/R_c = 0.8$

ACKNOWLEDGMENT

This work was supported by the Independent Research Fund of the Naval Surface Weapons Center and by the Department of Defense Advanced Research Projects Agency.

REFERENCES

1. J. G. Siambis and M. Friedman, Part. Accel. 8, 217 (1978).

2. D. B. McDermott, T. C. Marshall, S. P. Schlesinger, R. K. Parker, and V. L. Granatstein, Phys. Rev. Lett. 41, 1368 (1978).

3. H. S. Uhm and R. C. Davidson, Phys. Fluids, in press (1981).

4. G. Bekefi and T. J. Orzechowski, Phys. Rev. Lett. 37, 379 (1976).

5. V. A. Flyagin, A. V. Gaponov, M. I. Petelin, and V. K. Yulpatov, IEEE Trans. Microwave Theory Tech. MTT-25, 514 (1977).

6. H. S. Uhm and R. C. Davidson, Phys. Fluids 23, 2538 (1980).

7. J. Y. Choe, H. S. Uhm, and S. Ahn, J. Appl. Phys., in press (1981).

8. H. S. Uhm and J. G. Siambis, Phys. Fluids 22, 2237 (1979).

9. R. C. Davidson, Theory of Nonneutral Plasmas, (W. A. Benjamin, Inc., Reading, Mass., 1974), Ch. 2.

DISTRIBUTION

	Copies
Commander	
Naval Research Laboratory	
Attn: Dr. Saeyoung Ahn	1
Dr. Wahab A. Ali	1
Dr. J. M. Baird	1
Dr. L. Barnett	1
Dr. O. Book	1
Dr. Jay Boris	1
Dr. K. R. Chu	1
Dr. Timothy Coffey	1
Dr. G. Cooperstein	1
Dr. A. Drobot	1
Dr. Richard Fernslor	1
Dr. H. Freund	1
Dr. M. Friedman	1
Dr. J. Golden	1
Dr. S. Goldstein	1
Dr. V. Granatstein	1
Dr. Robert Greig	1
Dr. Irving Haber	1
Dr. Richard Hubbard	1
Dr. Bertram Hui	1
Dr. Glenn Joyce	1
Dr. Selig Kainer	1
Dr. C. A. Kapetanakos	1
Dr. M. Lampe	1
Dr. Y. Y. Lau	1
Dr. W. M. Manheimer	1
Dr. Don Murphy	1
Dr. Peter Palmadesso	1
Dr. Robert Pechacek	1
Dr. Michael Picone	1
Dr. Michael Raleigh	1
Dr. M. E. Read	1
Dr. C. W. Roberson	1
Dr. J. D. Sethian	1
Dr. William Sharp	1
Dr. J. S. Silverstein	1
Dr. Philip Sprangle	1
Dr. Doug Strickland	1
Dr. C. M. Tang	1
Dr. N. Vanderplaats	1
Washington, DC 20375	
Office of Naval Research	
Attn: Dr. Robert Behringer	1
1030 E. Green	
Pasadena, CA 91106	
Office of Naval Research	
Attn: Dr. T. Berlincourt	1
Dr. W. J. Condell	1
Department of the Navy	
Arlington, VA 22217	
Commander	
Naval Air Systems Command	
Attn: Dr. Wasneski	1
Department of the Navy	
Washington, DC 20361	
Commander	
Naval Sea Systems Command	
Attn: Dr. C. F. Sharn	1
Department of the Navy	
Washington, DC 20362	
Harry Diamond Laboratory	
Attn: Dr. H. E. Brandt	1
Dr. S. Graybill	1
2800 Powder Mill Road	
Adelphi, MD 20783	
U. S. Army Ballistic Research Laboratory	
Attn: Dr. D. Eccleshall	1
Aberdeen Proving Ground	
MD 21005	
Air Force Weapons Laboratory	
Attn: Dr. Ray Lemke	1
Kirtland Air Force Base	
Albuquerque, NM 87117	
Air Force Weapons Laboratory	
Attn: Dr. D. Straw	1
Kirtland AFB, NM 87117	

DISTRIBUTION (Cont.)

	Copies
U.S. Department of Energy	
Attn: Dr. T. Godlove	1
Dr. M. Month	1
Dr. J. A. Snow	1
Washington, DC 20545	
National Bureau of Standards	
Attn: Dr. Sam Penner	1
Bldg. 245	
Washington, DC 20234	
National Bureau of Standards	
Attn: Dr. Mark Wilson	1
Gaithersburg, MD 20760	
Defense Advanced Research Projects Agency	
Attn: Dr. J. Bayless	1
Dr. Robert Fossum	1
Dr. J. A. Mangano	1
LCOL W. Whitaker	1
1400 Wilson Blvd.	
Arlington, VA 22209	
Science Applications Inc.	
Attn: Dr. Richard E. Aamodt	1
934 Pearl St. Suite A	
Boulder, CO 80302	
Science Applications Inc.	
Attn: Dr. L. Feinstein	1
Dr. Robert Johnston	1
Dr. Douglas Keeley	1
Dr. John Siambis	1
5 Palo Alto Square	
Palo Alto, CA 94304	
Science Applications, Inc.	
Attn: Dr. A. W. Trivelpiece	1
San Diego, CA 92123	
Science Applications, Inc.	
Attn: Dr. Ron Parkinson	1
1200 Prospect Street	
P.O. Box 2351	
La Jolla, CA 92038	

	Copies
TRW	
Defense and Space Systems Group	
Attn: Dr. D. Arnush	1
Dr. M. Caponi	1
1 Space Park	
Redondo Beach, CA 90278	
Lawrence Livermore National Laboratory	
Attn: Dr. W. A. Barletta	1
Dr. R. Briggs	1
Dr. H. L. Buchanan	1
Dr. Frank Chambers	1
Dr. T. Fessenden	1
Dr. Edward P. Lee	1
Dr. James Mark	1
Dr. Jon A. Masamitsu	1
Dr. V. Kelvin Neil	1
Dr. R. Post	1
Dr. D. S. Prono	1
Dr. M. E. Rensink	1
Dr. Simon S. Yu	1
University of California	
Livermore, CA 94550	
Physics International Co.	
Attn: Dr. Jim Benford	1
Dr. S. Putnam	1
2700 Merced Street	
San Leandro, CA 94577	
Sandia Laboratories	
Attn: Dr. K. D. Bergeron	1
Dr. B. Epstein	1
Dr. S. Humphries	1
Dr. Tom Lockner	1
Dr. Bruce R. Miller	1
Dr. C. L. Olson	1
Dr. Gerold Yonas	1
Albuquerque, NM 87115	
La Jolla Institute	
Attn: Dr. K. Brueckner	1
Prof. N. M. Kroll	1
P.O. Box 1434	
La Jolla, CA 92038	

DISTRIBUTION (Cont.)

	Copies
Mission Research Corp.	
Attn: Dr. Neal Carron	1
Dr. Conrad Longmire	1
735 State Street	
Santa Barbara, CA 93102	
Mission Research Corp.	
Attn: Dr. B. Godfrey	1
1400 San Mateo Blvd, S.E.	
Suite A	
Albuquerque, NM 87108	
McDonnell Douglas Corp.	
Attn: Dr. M. Greenspan	1
Dr. J. Carl Leader	1
P. O. Box 516	
St. Louis, MO 63166	
Los Alamos National Lab.	
Attn: Dr. Barry Newberger	1
Dr. L. E. Thode	1
Mail Stop 608	
Los Alamos, NM 87544	
Los Alamos Scientific Lab.	
Attn: Dr. H. Dreicer	1
Dr. R. J. Faehl	1
Los Alamos, NM 87544	
Pulse Sciences, Inc.	
Attn: Dr. Sid Putnam	1
1615 Broadway, Suite 610	
Oakland, CA 94612	
National Science Foundation	
Attn: Dr. R. Hill	
Physics Division, #341	
Washington, DC 20550	
W. J. Schafer Associates, Inc.	
Attn: Dr. Edward Cornet	1
1901 North Fort Myer Dr.	
Arlington, VA 22209	

	Copies
Austin Research Associates	
Attn: Prof. W. E. Drummond	1
Dr. M. Lee Sloan	1
Dr. James R. Thompson	1
1901 Rutland Drive	
Austin, TX 78758	
Western Research Corporation	
Attn: Dr. Franklin Felber	1
8616 Commerce Avenue	
San Diego, CA 92121	
Jaycor	
Attn: Dr. J. U. Guillory	1
Dr. D. Tidman	1
205 S. Whiting Street	
Alexandria, VA 22304	
Varian Associates	
Attn: Dr. Howard Jory	1
611 Hansen Way	
Palo Alto, CA 94303	
Lawrence Berkeley Lab.	
Attn: Dr. Denis Keefe	1
Dr. Hogil Kim	1
Dr. Hong Chul Kim	1
Dr. Kwang Je Kim	1
Dr. L. J. Laslett	1
Dr. G. R. Lambertson	1
Dr. A. M. Sessler	1
Dr. L. Smith	1
1 Cyclotron Road	
Berkeley, CA 94720	
Stanford Linear Accelerator Center	
Attn: Dr. Philip Morton	1
P.O. Box 4349	
Stanford, CA 94305	
AVCO - Everett Research Laboratory, Inc.	
Attn: Dr. Richard Patrick	1
2385 Revere Beach Pkwy	
Everett, MA 02149	

DISTRIBUTION (Cont.)

	Copies
Oak Ridge National Lab	
Attn: Dr. J. A. Rome	1
Oak Ridge, TN 37850	
University of California at Los Angeles	
Attn: Prof. F. Chen	1
Dr. A. T. Lin	1
Dr. J. Dawson	1
Dr. C. S. Liu	1
Dr. Edward Ott	1
Los Angeles, CA 90024	
University of Maryland	
Attn: Dr. W. Destlar	1
Dr. C. S. Liu	1
Dr. Won Namkung	1
Dr. E. Ott	1
Prof. M. Reiser	1
Dr. Moon-Jhong Rhee	1
Dr. C. D. Striffler	1
College Park, MD 20742	
Columbia University	
Attn: Prof. P. Diament	1
Prof. S. Schlesinger	1
New York, NY 10027	
North Carolina State University	
Attn: Prof. W. Doggett	1
Dr. Jin Joong Kim	1
P. O. Box 5342	
Raleigh, NC 27650	
Massachusetts Institute of Technology	
Attn: Prof. George Bekefi	1
Dr. K. J. Button	1
Prof. R. Davidson	1
Dr. R. Temkin	1
77 Massachusetts Avenue	
Cambridge, MA 02139	
University of California	
Attn: Dr. Gregory Benford	1
Dr. A. Fisher	1
Prof. N. Rostoker	1
Physics Department	
Irvine, CA 92717	
Yale University	
Attn: Dr. I. B. Bernstein	1
Dr. J. L. Hirshfield	1
Mason Laboratory	
400 Temple Street	
New Haven, CT 06520	
Cornell University	
Attn: Prof. H. Fleischmann	1
Prof. D. Hammer	1
Prof. R. V. Lovelace	1
Prof. J. Nation	1
Prof. R. Sudan	1
Ithaca, NY 14850	
University of Texas at Austin	
Attn: Dr. M. N. Rosenbluth	1
Institute for Fusion Studies	
RLM 11.218	
Austin, TX 78712	
Stevens Institute of Technology	
Attn: Prof. George Schmidt	1
Physics Department	
Hoboken, NJ 07030	
Dartmouth College	
Attn: Dr. John E. Walsh	1
Department of Physics	
Hanover, NH 03755	
Defense Technical Information Center	
Cameron Station	
Alexandria, VA 22314	12

DATE
FILMED

5-8